Cortactin Is an Essential Regulator of Matrix Metalloproteinase Secretion and Extracellular Matrix Degradation in Invadopodia

Emily S. Clark,[1] Amy S. Whigham,[2] Wendell G. Yarbrough,[2,3] and Alissa M. Weaver[1,3]

Departments of [1]Pathology, [2]Otolaryngology, and [3]Cancer Biology, Vanderbilt University, Nashville, Tennessee

Abstract

Invadopodia are branched actin-rich structures associated with extracellular matrix (ECM) degradation that collectively form the invasive machinery of aggressive cancer cells. Cortactin is a prominent component and a specific marker of invadopodia. Amplification of cortactin is associated with poor prognosis in head and neck squamous cell carcinomas (HNSCC), possibly because of its activity in invadopodia. Although the role of cortactin in invadopodia has been attributed to signaling and actin assembly, it is incompletely understood. We made HNSCC cells deficient in cortactin by RNA interference knockdown methods. In these cortactin knockdown cells, invadopodia were reduced in number and lost their ability to degrade ECM. In the reverse experiment, overexpression of cortactin dramatically increased ECM degradation, far above and beyond the effect on formation of actin/Arp3–positive invadopodia puncta. Secretion of matrix metalloproteinases (MMP) MMP-2 and MMP-9, as well as plasma membrane delivery of MT1-MMP correlated closely with cortactin expression levels. MMP inhibitor treatment of control cells mimicked the cortactin knockdown phenotype, with abolished ECM degradation and fewer invadopodia, suggesting a positive feedback loop in which degradation products from MMP activity promote new invadopodia formation. Collectively, these data suggest that a major role of cortactin in invadopodia is to regulate the secretion of MMPs and point to a novel mechanism coupling dynamic actin assembly to the secretory machinery, producing enhanced ECM degradation and invasiveness. Furthermore, these data provide a possible explanation for the observed association between cortactin overexpression and enhanced invasiveness and poor prognosis in HNSCC patients. [Cancer Res 2007;67(9):4227–35]

Introduction

The ability to degrade extracellular matrix (ECM) is a hallmark of invasive tumors and is thought to be essential for the movement of cancer cells through tissue barriers (1, 2). At the subcellular level, ECM-degrading activity has been associated with finger-like, actin-rich protrusions, known as invadopodia (3, 4). Similar structures, termed podosomes, are formed by a number of normal cell types that need to cross tissue barriers or remodel matrix, including osteoclasts, smooth muscle cells, and macrophages (5). Invadopodia and podosomes share many structural and functional characteristics, including a dependence on branched actin assembly and src kinase signaling, as well as common molecular components (4, 5).

In many ways, invadopodia are similar to lamellipodia, which are two-dimensional branched actin-filled membrane protrusions that form at the leading edge of migrating cells and direct cell movement. In analogy to lamellipodia, branched actin assembly nucleated by the Arp2/3 complex is thought to be an initiating event for invadopodia formation (6). Key actin assembly molecules that regulate invadopodia include N-WASp, Arp2/3 complex, WAVE1, cortactin, gelsolin, and cofilin (7–15). However, invadopodia have a number of unique aspects, including the absolute dependence on src kinase signaling, the presence of focal adhesion proteins in the same location as branched actin, and the localization of active matrix degradation to sites of invadopodia formation (4, 5). How the diverse processes of actin assembly, signaling, and membrane trafficking for protease secretion and cell-matrix adhesion are integrated to produce a functional ECM-degrading machine is poorly understood.

Tumor cells frequently overexpress matrix metalloproteinases (MMP) and this has been correlated with invasive capacity, metastatic potential, and/or poor prognosis in a number of cancers, including prostate, stomach, lung, colon, breast, ovary, thyroid, and head and neck squamous cell carcinoma (HNSCC; ref. 16). MMP-1, MMP-2, MMP-9, and MT1-MMP (MMP-14) have been most commonly identified with HNSCC and associated with disease progression (17). The matrix-degrading capability of invadopodia has been mostly attributed to MMPs, including MT1-MMP, MMP-2, MMP-9, and metalloproteinases of the ADAM family (18–21). The serine proteinase seprase has also been linked to invadopodia function (4, 22). MMPs are produced as pro-enzymes, and are either proteolytically activated en route to the plasma membrane from the *trans*-Golgi network (MT1-MMP) or after secretion (MMP-2 and MMP-9; refs. 20, 23–25). The localization of ECM-degrading activity to invadopodia could be due to several factors, including protection from inactivators of proteinase activity (19) and the concentration of ECM-degrading proteases at invadopodia foci (7, 19, 21, 26, 27).

Cortactin is an actin-binding protein that has been receiving particular interest in the invadopodia field (7, 9, 10, 28). Cortactin was first identified as a prominent src tyrosine kinase substrate and was later shown to regulate Arp2/3 complex activity (29–31). In addition to src kinase, Arp2/3, and actin filaments, cortactin binds a number of additional proteins, including dynamin2, N-WASp, WIP, Erk kinase, Shank, and MLCK (32). The *cortactin* gene within the 11q13 amplicon is frequently amplified in a number of human cancers. *Cortactin* gene amplification has been tied to poor prognosis in HNSCC (33–35). Consistent with a role in cancer aggressiveness, we and others have shown that cortactin promotes motility and invasiveness of cells (36–38) and regulates lamellipodial stability, membrane trafficking, and cell-cell adhesion

Note: Supplementary data for this article are available at Cancer Research Online (http://cancerres.aacrjournals.org/).

Requests for reprints: Alissa M. Weaver, Department of Cancer Biology, Vanderbilt University, Nashville, TN 37232. Phone: 615-936-3529; Fax: 615-936-2911; E-mail: alissa.weaver@vanderbilt.edu.

doi:10.1158/0008-5472.CAN-06-3928

(36, 39, 40). In the majority of studies, cortactin function has been tied to regulation of Arp2/3 complex activity. However, many actions of cortactin are likely to involve interactions with the more than 20 cortactin-binding partners. In particular, cortactin has the potential to link several invadopodia processes, including actin assembly, src kinase signaling, and membrane trafficking (4, 10, 15, 28, 41).

Cortactin has been shown to be a regulator of podosome/invadopodia formation in osteoclasts, vascular smooth muscle cells, and breast cancer cells (7, 9, 28, 42). The role of cortactin in invadopodia has been typically attributed to regulation of branched actin assembly, based on the fact that cortactin stabilizes Arp2/3-mediated actin branches and is a cofactor in Arp2/3 activation (29, 31). We examined the role of cortactin in invadopodia function in HNSCC cells. Surprisingly, we find that cortactin is essential for invadopodia-associated ECM degradation and has a lesser effect on formation of actin- and Arp2/3-labeled invadopodia puncta (i.e., cells exhibit a reduced number of invadopodia). In addition, we find that cortactin regulates the secretion of invadopodia-associated MMPs: MMP-2, MMP-9, and MT1-MMP. Interestingly, inhibition of MMPs leads to a decrease in invadopodia actin puncta formation to a degree similar to that of cortactin shRNA. These data suggest that a major role of cortactin in invadopodia is to regulate the secretion of MMPs and that at least part of the reduction in invadopodia formation by cortactin may be due to interruption of a positive feedback loop from MMP activity.

Materials and Methods

Antibodies and chemicals. Antibodies against MMP-2, MMP-9, and MT1-MMP were from Chemicon International; anti-Arp3 has been previously described (43); monoclonal anticortactin antibody for immunofluorescence was 4F11 (Upstate); polyclonal anticortactin antibody for Western blotting was previously described (36); anti–β-actin was from Sigma (AC-74); anti–cyclophilin B antibody was from Alexis Biochemicals; and anti-apolipoprotein A1 (ApoA1) antibody was a gift from Larry Swift (Vanderbilt University). All fluorescently labeled secondary antibodies, phalloidin, and CellTracker Red were from Invitrogen. GM6001 and human recombinant tissue inhibitor of metalloproteinase-2 (TIMP-2) were from Calbiochem.

Construction of small interfering RNA and retroviral expression constructs. The 64-bp oligonucleotides containing sense and antisense sequences flanking a 6-bp hairpin have been described previously (36). The 19-base sequence to construct pRetroSuper (pRS)-KD1 was targeted to nucleotides 552 to 570 of human cortactin, GCACGAGTCACAGAGAGAT. pRS-KD2 was constructed by targeting nucleotides 343 to 361 using the sequence AAGCTGAGGGAGAATGTCT. All oligonucleotides were purchased from Integrated DNA Technologies. The oligonucleotides were inserted into the pRS vector (a kind gift of Reuven Agami, Division of Tumor Biology, The Netherlands Cancer Institute, Amsterdam, the Netherlands; ref. 44). Cortactin constructs for overexpression or reexpression were cloned into LZRS-Neo retroviral expression vector (45). Phoenix 293 packaging cells (from Garry Nolan, Department of Microbiology and Immunology, Stanford University, Stanford, CA) were maintained in DMEM supplemented with 10% heat-inactivated bovine growth serum (Hyclone). Phoenix 293 cell transfection, viral harvest, and target cell transduction were done as previously described (45). Cells were selected with 4 μg/mL puromycin or 600 μg/mL G418 for expression of pRS or LZRS, respectively.

Cell culture. The HNSCC cell lines SCC61 and SCC25 were obtained from Wendell Yarbrough (Vanderbilt University). Both cell lines were isolated from tongue squamous cell carcinoma tumors and considered aggressive, as defined by lack of response to radiation therapy and the presence of tumor-positive lymph nodes (46). The SCC61 tumor was stage $T_{4x}N_{2BX}$ and the SCC25 tumor was stage T_2N_1 according to the American Joint Committee for Cancer Staging and End Result Reporting guidelines. SCC61 cells were maintained in DMEM supplemented with 20% fetal bovine serum (FBS) and 0.4 μg/mL hydrocortisone. SCC25 cells were maintained in DMEM/F12 supplemented with 20% FBS. Primary human HNSCC tumors were obtained at the time of biopsy or surgical resection under institutional review board (IRB)–approved protocols (IRB 030062 and 050259). Tumors were washed in 1% povodine iodine and then digested with 0.05% trypsin for 3 h at 37°C (47). Cells were strained to remove debris, washed, and cultured for the *in vitro* matrix degradation assay (described below).

Western blot analyses. For blots of whole-cell lysates, equal numbers of cells were lysed directly in 4× Laemmli sample buffer [0.2 mol/L Tris (pH 7.0), 4% SDS, 20% glycerol, 0.16 mol/L DTT, and protease inhibitor cocktail (Sigma)], boiled, and separated by electrophoresis on 10% SDS-PAGE gels. For analysis of conditioned medium, samples were collected as for zymography (see below), but boiled in reducing Laemmli sample buffer and analyzed on 10% SDS-PAGE gels. Proteins were transferred to nitrocellulose and blocked in 5% milk in TBS + 0.1% Tween 20 (TBST). After the appropriate antibody incubations, blots were developed by enhanced chemiluminescence and exposed to X-ray film or scanned using the Odyssey Infrared Scanner. β-Actin and the noncytoskeletal protein cyclophilin B were used as loading controls (graphs in Fig. 2*A* and Supplementary Fig. S2*A*; normalized using cyclophilin B levels). Densitometry was done using ImageJ software (NIH) or Odyssey software. All densities are shown as values normalized to cyclophilin B expression and then as percentage of expression of the pRS control.

***In vitro* matrix degradation assay.** The matrix degradation assay was done as described by Chen et al. (48). Briefly, fibronectin (BD Biosciences) was labeled with FITC (Sigma) by dialysis in borate buffer [0.17 mol/L borate, 0.075 mol/L NaCl (pH 9.3)]. The buffer was changed to PBS and dialyzed extensively for 3 to 4 days, followed by dialysis against 50% glycerol in PBS and storage at −20°C. To coat MatTek dishes, 2.5% gelatin/2.5% sucrose in PBS was heated to 37°C and added to the dish, followed by cross-linking with 0.5% glutaraldehyde in PBS. After ultracentrifugation at 70,000 rpm for 15 min to remove aggregates, a 50 μg/mL solution of FITC-fibronectin was prepared in PBS and incubated with the cross-linked gelatin in MatTek dishes in the dark for 1 h. The dish was sterilized with 70% ethanol, washed with DMEM, and equilibrated with invadopodia medium [DMEM supplemented with 20% FetalClone III (Hyclone) and 10% Nu-Serum (Invitrogen)] for 30 min before the addition of cells. For invadopodia assays, 5×10^4 cells were suspended in 2 mL of invadopodia medium and added to the plate for 20 h (cell lines) or 36 h (primary tumor cells). The cells were fixed in 3% paraformaldehyde in PIPES buffer (127 mmol/L NaCl, 5 mmol/L KCl, 1.1 mmol/L NaH_2PO_4, 0.4 mmol/L KH_2PO_4, 2 mmol/L $MgCl_2$, 5.5 mM glucose, 1 mmol/L EGTA, and 20 mmol/L PIPES), permeabilized with 0.4% Triton X-100 in PBS, or fixed and permeabilized with ice-cold methanol and blocked with 3% bovine serum albumin (BSA) in PBS + 0.1% Tween 20 and incubated with appropriate primary and secondary antibodies or fluorescent phalloidin.

Microscopy and image analysis. Images were captured using a Nikon Eclipse TE2000-E wide-field fluorescent microscope equipped with a ×40 Plan Fluor 1.3 numerical aperture (NA) objective or a Zeiss LSM510 Meta with a ×40 Plan-NeoFluar 1.3 NA objective (Fig. 1; Tumor 2; Vanderbilt Cell Imaging Shared Resource). At least 10 randomly chosen fields were imaged per trial. Image analysis was done using Metamorph. Invadopodia were manually counted and graphed as either number of invadopodia per cell or the percentage of cells with invadopodia. Invadopodia were defined as actin puncta that were also positive for either cortactin (Fig. 1) or Arp3 (all other figures). In addition, to be counted, invadopodia needed to be ≥1 μm in diameter. Cell area was determined by tracing the cell footprint of the β-actin channel and using region tools to calculate area. The calculation for cell area was compared between β-actin and the cytoplasmic dye, CellTracker Red, and found to not be significantly different (data not shown). Therefore, to be able to determine cell area and to visualize invadopodia in the same fluorescent channel, actin staining was used. Degradation area was determined by performing an inclusive threshold of the FITC channel to include the dark, degraded areas; then, region tools were used to calculate the thresholded area. Data were collected in an Excel spreadsheet and used to calculate degradation area per cell area.

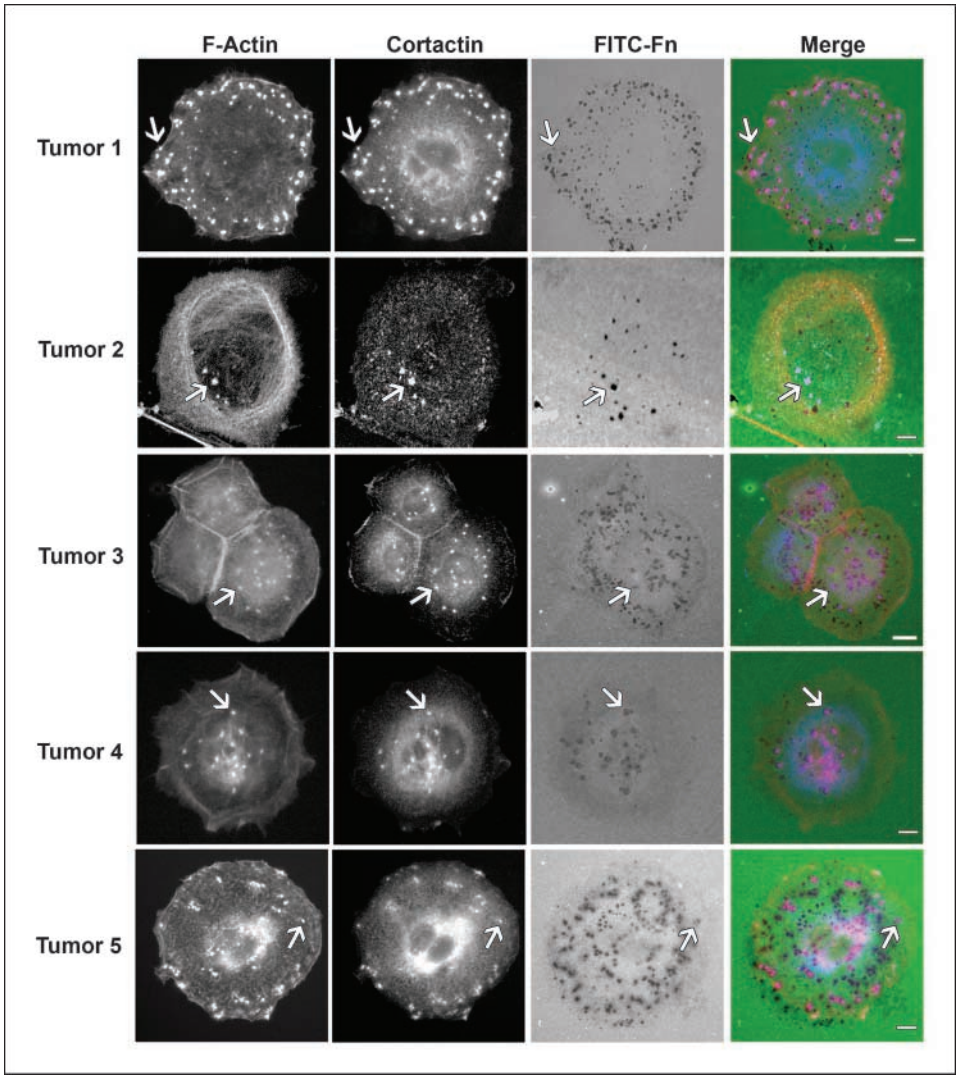

Figure 1. Primary human HNSCC tumors form invadopodia. Biopsy-confirmed human HNSCC tumors were surgically removed, and single-cell suspensions were prepared and cultured on glass coverslips covered with cross-linked gelatin overlaid with FITC-fibronectin (*FITC-Fn*). Cells were stained with phalloidin to identify actin filaments (F-actin; *red in Merge*) and with 4F11 anticortactin antibody (*blue in Merge*). Degraded ECM is identified as a dark area on the FITC-fibronectin (*green in Merge*) background. *Pink in Merge,* colocalization of cortactin and actin staining. *Yellow in Merge,* colocalization of actin with nondegraded ECM. *Turquoise,* colocalization of cortactin with nondegraded ECM. *White,* colocalization of all three colors. *Arrows,* an example invadopodia, identified as actin and cortactin-positive puncta overlying areas of cell-associated ECM degradation. Representative images from cells prepared from tumors. $n = 5$. *Bar,* 10 μm.

Gelatin zymography. Samples for gelatin zymography were prepared as previously described (49, 50). Briefly, 2×10^5 cells were plated per well of a 24-well plate in complete growth medium. After overnight incubation, the cells were washed twice with PBS and 300 μL of serum-free medium was added to each well and incubated for various time points, up to 48 h. Control cell counting experiments were done to ensure that all cell lines had equivalent growth rates over the experimental time points and that equal numbers of cells were present in each well. A 40 μL aliquot of conditioned medium was mixed with nonreducing sample buffer [250 mmol/L Tris (pH 6.8), 25% glycerol, 10% SDS, and 0.01% bromphenol blue], incubated for 15 min at 37°C, and loaded in a 10% SDS-PAGE gel containing 0.25% gelatin. A positive control sample of medium containing 10% FBS was used. Following electrophoresis, the gel was washed twice for 15 min each in 2.5% Triton X-100 and incubated for either 24 h (Fig. 4*A* and *B*) or 48 h (Fig. 4*C*) at 37°C in substrate buffer [50 mmol/L Tris, 10 mmol/L $CaCl_2$ (pH 7.6)]. After incubation, the gel was stained with 0.5% Coomassie blue R250 in 50% methanol, 10% acetic acid. Gels were destained briefly in 50% methanol, 10% acetic acid, and then in water. Areas of gelatinase activity appeared clear on the Coomassie-stained gel. Following destaining, gels were scanned using the Odyssey Infrared Scanner and densitometry was done using the Odyssey software. MMP levels for each data point are internally normalized to the levels of MMP for the zero time point on the same gel and thus plotted as the fold increase with respect to the levels at $t = 0$.

Fluorescence-activated cell sorting analysis. Cells (1×10^6) were cultured overnight in a six-well plate, collected with 5 mmol/L EDTA in PBS, and surface labeled with an antibody against MT1-MMP and the appropriate AlexaFluor-488–conjugated secondary antibody. Specifically, cells were blocked with 3% BSA in TBST for 1 h, incubated with primary antibody, washed thrice with PBS, incubated with the appropriate AlexaFluor-488 secondary antibody, and washed an additional three times with PBS. To ensure surface labeling, all solutions were ice-cold and the cells were kept on ice during all incubation steps. Following staining, cells were fixed in 2% paraformaldehyde and kept in the dark until analysis. Control cells were stained in parallel with secondary antibody only to reveal background. Analysis was done using the LSRII Flow Cytometer (BD Biosciences) at the Vanderbilt University Medical Center Flow Cytometry Core Facility. The mean fluorescence intensity for the control cells (secondary staining only) was subtracted from the mean fluorescence intensity for each cell line, and the results are graphed as percentage of expression relative to the pRS [vector only control for small interfering (siRNA)] cell line.

Statistical analyses. Excel was used to calculate means and SE. Prism InStat was used to perform statistical tests of significance. Comparison between two groups (all figures except Supplementary Fig. S4) was done using the unpaired Student's t test. Multiple comparisons (Supplementary Fig. S4) were done by ANOVA. Statistical significance was set at $P < 0.05$.

Results

Primary HNSCC tumor cells form invadopodia and degrade ECM. We obtained primary tumor cells from patients

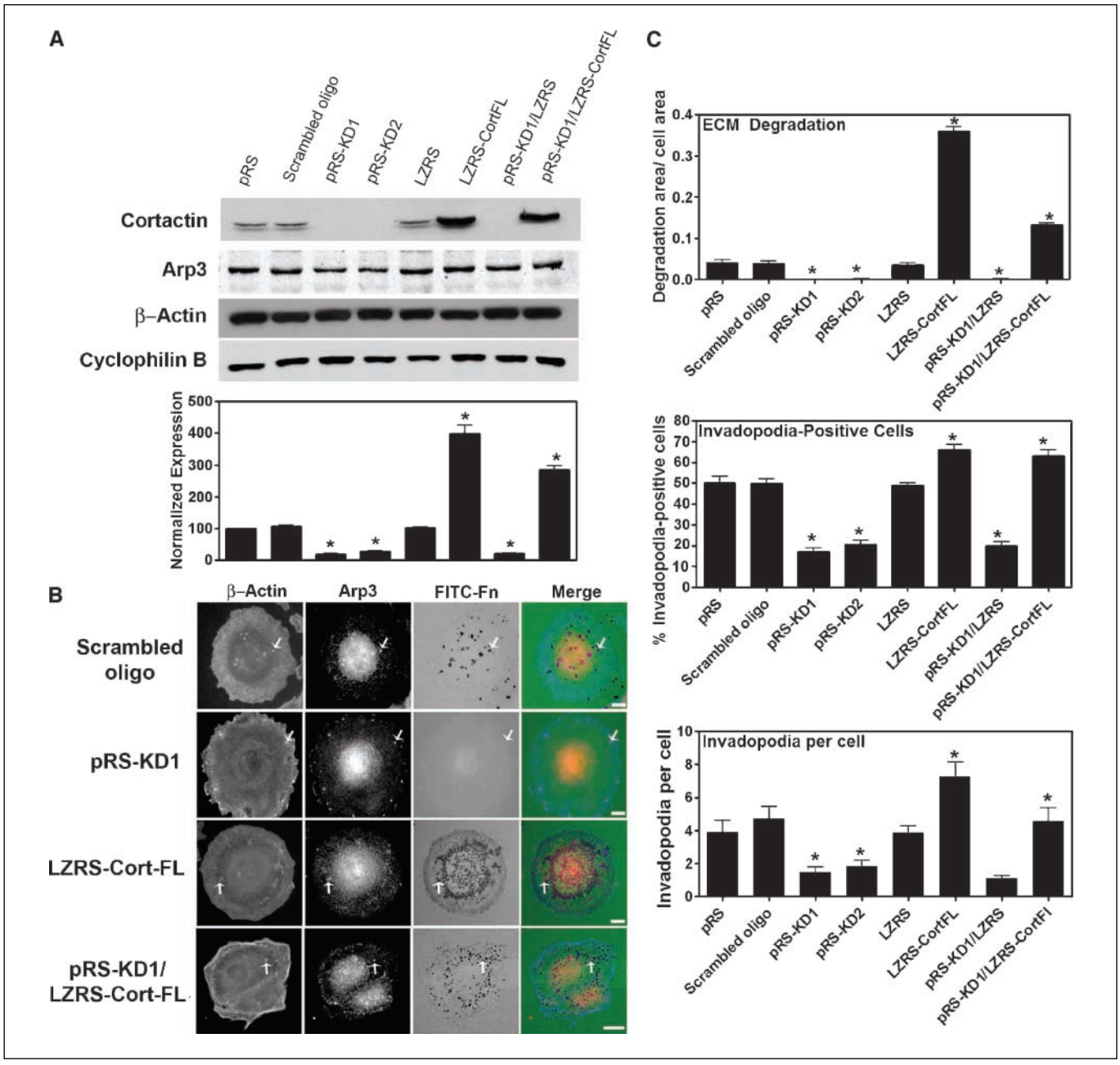

Figure 2. Cortactin regulates invadopodia-mediated ECM degradation more than invadopodia formation. *A,* representative Western blot and densitometry of cortactin expression in SCC61 cells in shRNA vector control (*pRS*), scrambled cortactin siRNA oligonucleotide (*Scrambled oligo*), cortactin knockdown cells (*pRS-KD1* and *pRS-KD2*), overexpression vector control (*LZRS*), cortactin-overexpressing cells (*LZRS-CortFL*), knockdown cells rescued with vector only (*pRS-KD1/LZRS*), and knockdown cells rescued with full-length mouse cortactin (*pRS-KD1/LZRS-CortFL*). The blots were reprobed for Arp3, β-actin, and cyclophilin B and show no changes in expression. Densitometry of cortactin expression normalized to cyclophilin B expression from three separate Western blots is also shown. Data are represented as percentage of expression relative to pRS control. *Columns,* mean ($n = 3$); *bars,* SE. *B,* representative images from the *in vitro* matrix degradation assay. Cells are cultured for 20 h on gelatin overlaid with FITC-fibronectin, fixed, and stained with antibodies against β-actin (*blue in Merge*) and Arp3 (*red in Merge*) to localize invadopodia. *Pink in Merge,* colocalization between Arp3 and actin. *Yellow,* colocalization between Arp3 and FITC-fibronectin. *Turquoise,* colocalization between actin and FITC-fibronectin. *White,* colocalization of all three signals. *Bar*, 10 μm. *Arrows,* an example invadopodia in each cell. Note the lack of matrix degradation associated with cortactin knockdown invadopodia. For images of additional cell lines and multiple images of control cells, see Supplementary Figs. S1 and S2. *C, in vitro* matrix degradation assay with quantification of matrix-degrading capability (*top*), percentage of cells with invadopodia (*middle*), and number of invadopodia per cell (*bottom*). Invadopodia were identified by puncta that exhibited double-positive staining for β-actin and Arp3. Quantification from three independent experiments, 10 to 12 fields for each cell line per experiment. *Columns,* mean; *bars,* SE. *, $P < 0.05$, compared with pRS control. An analysis of invadopodia diameter for control and knockdown cells is shown in Supplementary Fig. S2.

with biopsy-confirmed HNSCC, prepared single-cell suspensions, and tested them for invadopodia formation within 4 h of harvesting by plating them on cross-linked gelatin overlaid with FITC-fibronectin for 36 h. Samples were randomly selected, without bias for anatomic site, stage, or histologic features. Interestingly, all five tumor samples tested formed invadopodia and degraded ECM, consistent with the generally invasive phenotype of HNSCC tumors and noted *in vivo* invasion of these

specific tumors (Fig. 1; information on tumor characteristics and clinical stage is available in Supplementary Table S1). Cells were considered to be positive for invadopodia formation if they had actin-rich puncta in the cell that also stained for cortactin and were overlying areas of cell-associated matrix degradation. Because some invadopodia are dynamic, especially in migrating cells (7, 14), areas of degradation can also be seen that are no longer associated with corresponding invadopodia.

Cortactin promotes invadopodia-associated matrix degradation more than the formation of invadopodia. To test the role of cortactin in HNSCC invadopodia function, we switched to a more genetically tractable system than primary tumors—HNSCC cell lines. A retroviral shRNA expression system, pRS, was used to stably knock down cortactin in SCC61 HNSCC cells (Fig. 2*A*). Both human cortactin-targeted siRNA sequences contained mismatches with the orthologous murine gene, to allow for rescue with mouse cortactin. Cortactin expression was almost completely abolished in two separate stable, polyclonal cell populations: pRS-KD1 and pRS-KD2. The LZRS retroviral expression system was used to overexpress (LZRS-CortFL) or reexpress mouse cortactin in the knockdown background (pRS-KD1/LZRS-CortFL; Fig. 2*A*).

To test the role of cortactin in invadopodia function, HNSCC cells were cultured overnight on MatTek dishes coated with FITC-fibronectin/gelatin substrate, and fixed and stained for invadopodia, this time with antibodies against β-actin and Arp3, because cortactin could no longer be used as an invadopodia marker in all cell lines (Fig. 2*B*; Supplementary Figs. S1 and S2). Expression levels for both β-actin and Arp3 were determined to be equal for all cell lines by Western blot analysis (Fig. 2*A*). Quantification of three measurements, ECM degradation per cell, the percentage of cells with invadopodia puncta, and the number of invadopodia puncta per cell, was done as described in Materials and Methods. Consistent with previous results (7, 9, 28, 42), cortactin is important for invadopodia formation. The percentage of cells with Arp3-positive actin puncta is reduced by >2-fold in cortactin-deficient cell lines and is slightly increased in cells that overexpress cortactin (Fig. 2*C*). Quantification of the number of invadopodia per cell gives similar results to quantification of the percentage of invadopodia-positive cells (Fig. 2*C*). To determine whether there was a change in the size of individual invadopodia, we also measured the diameter of invadopodia from control and cortactin knockdown cells and found that there was no difference (Supplementary Fig. S2). Surprisingly, cortactin expression has a greater effect on invadopodia-associated ECM degradation than on the formation of invadopodia. FITC-fibronectin degradation is increased by 6- to 7-fold when cells overexpress cortactin, whereas cortactin-deficient cells completely lose the ability to degrade ECM (Fig. 2*C*). This result is evident in multiple HNSCC cell lines

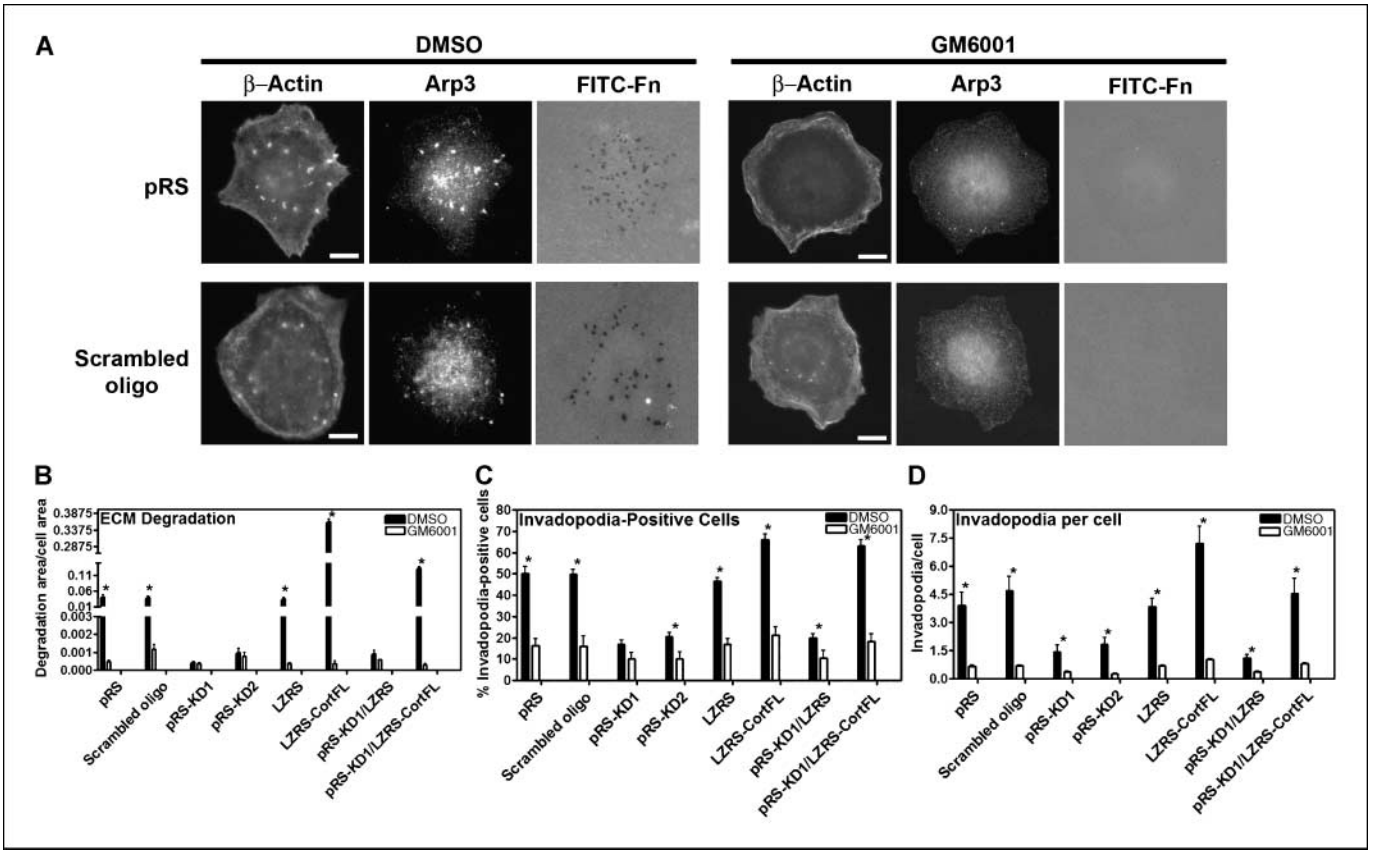

Figure 3. Inhibition of MMP activity inhibits invadopodia formation. The *in vitro* matrix degradation assay was done in the presence of 25 μmol/L GM6001, a general MMP inhibitor (*open columns*) or DMSO diluent (*closed columns*). *A,* representative images of pRS (*top*) or scrambled shRNA (*bottom*) control cells treated with either vehicle (DMSO) or 25 μmol/L GM6001, as labeled. *Bar,* 10 μm. *B,* ECM degradation. *C,* percentage of cells with invadopodia formation. *D,* invadopodia per cell was quantified. There was no associated toxicity with this concentration of inhibitor, as verified by trypan blue exclusion (data not shown). Quantification from three independent experiments, 10 to 12 fields for each cell line per experiment. *Solid columns,* DMSO treatment; *open columns,* GM6001 treatment. *Columns,* mean; *bars,* SE. *, $P < 0.05$, comparing DMSO diluent with GM6001 for each cell line.

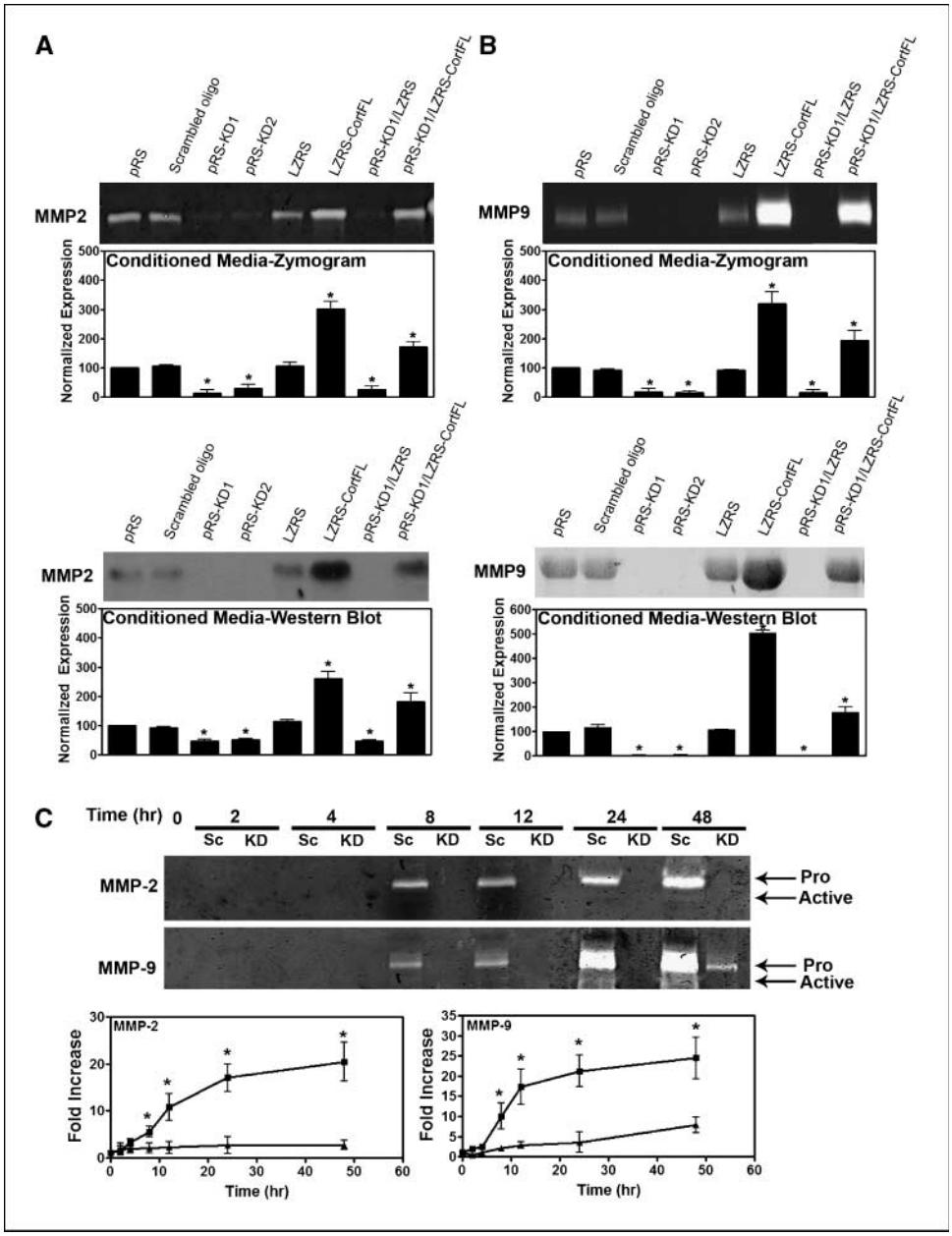

Figure 4. Cortactin expression affects secretion of MMP-2 and MMP-9. *A* and *B,* representative zymograms and Western blots from 24 h conditioned medium showing secretion of MMP-2 (*A*) and MMP-9 (*B*) and combined densitometric measurements from three separate experiments. Equal volume (40 μL) of conditioned medium collected from wells with equal cell number was loaded into each well. *Columns,* mean; *bars,* SE. *, $P < 0.05$, compared with pRS control. *C,* representative zymogram of conditioned medium (40 μL) from scrambled oligonucleotide (*Sc*) and pRS-CortKD1 (*KD*) cells. Equal numbers of cells (2.0×10^5) were plated per well for each corresponding time point in 300 μL of serum-free medium. At each time, the medium was collected. The zero time point is 40 μL of serum-free medium. *Graphs,* fold increase over the zero time point for MMP-2 and MMP-9 secretion from three independent experiments. *Points,* mean; *bars,* SE. *, $P < 0.05$, compared with control for that time point.

(results from SCC25 cells shown in Supplementary Fig. S3; data from SCC47 and SQ20B not shown). The defect in cortactin knockdown cells is fully rescued by reexpression of cortactin (Fig. 2; Supplementary Figs. S1 and S3). These data suggest that the role of cortactin in invadopodia may not be limited to the initial actin assembly phase but may also include regulation of ECM degradation.

Inhibition of MMPs phenocopies the effect of cortactin knockdown on invadopodia function. To test the role of ECM-degrading metalloproteinases in our system, we measured the ability of SCC61 cells to form invadopodia and degrade matrix in the presence of the general MMP and ADAM inhibitor GM6001. As shown in Fig. 3*A* and *B*, incubation of cells with 25 μmol/L GM6001 completely ablates matrix degradation by all of the cell lines. Surprisingly, GM6001 also reduces the ability of cells to form invadopodia, as measured by both the percentage of cells that form invadopodia and the number of invadopodia per cell (Fig. 3*C* and *D*). Strikingly, GM6001 reduces both invadopodia formation and ECM degradation in control cells to approximately the same level seen in cortactin knockdown cells, suggesting that cortactin may function in invadopodia to modulate MMP and/or ADAM proteinase expression or activity. To more specifically determine whether cortactin affects MMPs versus ADAM proteinases, control (pRS and scrambled oligonucleotide) cells were treated with 0.3 μg/mL human recombinant TIMP-2, a biological MMP inhibitor that is not to our knowledge known to affect ADAMs (51, 52). Both GM6001 and TIMP-2 gave equivalent results, including reduction in the number of invadopodia per cell (Supplementary Fig. S4). Thus, although we cannot fully rule out effects of cortactin on expression or activity of other ECM-degrading proteinases, such as ADAMs in invadopodia, our data point to MMPs as the most likely candidates to be regulated by cortactin.

Cortactin promotes MMP secretion. To determine the role of cortactin in MMP activity in invadopodia, we quantified the relative levels of the major MMPs associated with invadopodia function in cortactin-manipulated SCC61 cells. First, we did Western blot analyses of whole-cell lysates and found no alteration in expression levels of MMP-2 or MMP-9 protein (data not shown). However, because MMPs function in the extracellular space, delivery to the plasma membrane and secretion is another potential mechanism for regulation of MMP activity. To test whether cortactin expression modulates MMP-2 and MMP-9 secretion, we did both gelatin zymography and Western blot analyses on conditioned medium samples collected from SCC61 cells. As shown in Fig. 4*A* and *B*, overexpression of cortactin causes an increase in the levels of MMP-2 and MMP-9 in 24-h conditioned medium samples, whereas cells that are deficient in cortactin had no detectable MMP-9 (Fig. 4*B*) and very little MMP-2 (Fig. 4*A*) in 24-h conditioned medium samples. To rule out the possibility that changes in MMP-2 and MMP-9 levels were due to a process other than secretion, such as altered stability or increased degradation postsecretion, conditioned medium was collected over a 48-h time course and analyzed by zymography. MMP-2 and MMP-9 were detectable in control medium beginning at 8 h and accumulated steadily over time. By contrast, no MMP was detectable in cortactin knockdown conditioned medium at any of the time points, except for a small amount of MMP-9 at 48 h (Fig. 4*C*). These data strongly suggest that cortactin knockdown cells have a MMP secretion defect. To determine whether cortactin affects secretion generally, conditioned medium from the 24-h samples was analyzed for the presence of ApoA1, a protein that is secreted by many cancer cells but is irrelevant to invadopodia (53). Cells deficient in cortactin are also impaired for secretion of ApoA1, indicating that these cells may have a broad secretion defect phenotype (Supplementary Fig. S5).

MT1-MMP is a transmembrane metalloproteinase that has been closely connected to ECM degradation by invadopodia as well as to poor prognosis of tumors (16, 21, 54). Examination of MT1-MMP expression by Western blot also showed that cortactin does not affect the overall MT1-MMP expression level in whole-cell lysates (data not shown). To detect changes in the trafficking of MT1-MMP, we stained cells for surface MT1-MMP expression and analyzed them by flow cytometry. Similar to the results with MMP-2 and MMP-9, cortactin knockdown cells exhibit a decrease, whereas cortactin-overexpressing cells (LZRS-Cort-FL and pRS-KD/LZRS-CortFL) show an increase, in MT1-MMP cell surface expression (Fig. 5). Collectively, these data indicate that cortactin modulates the secretion and extracellular surface expression of key invadopodia-associated MMPs, including the transmembrane protein MT1-MMP.

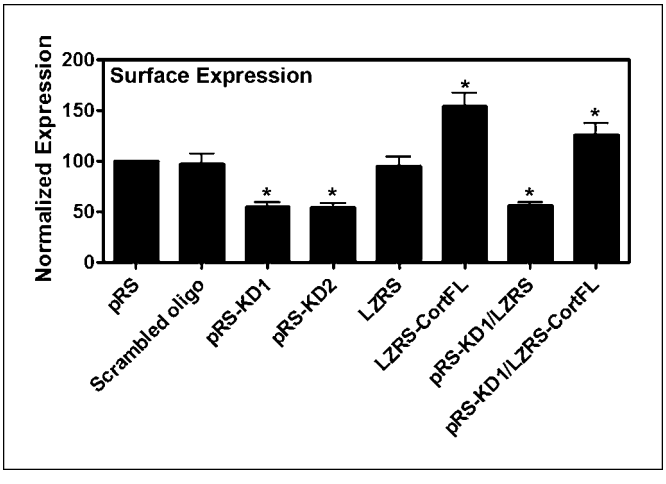

Figure 5. Cortactin expression affects the cell surface expression of MT1-MMP. *A,* fluorescence-activated cell sorting analysis of surface expression of MT1-MMP from three independent experiments. Each value is background subtracted and graphed relative to pRS control. *Columns,* mean; *bars,* SE. *, $P < 0.05$.

Discussion

HNSCC is a particularly invasive type of cancer, with much of the morbidity caused from local invasion into vital structures such as central nerves and vessels concentrated in the neck and structures of the upper aerodigestive tract (55). In this study, we examined the role of *cortactin*, a candidate oncogene in the 11q13 amplicon that has been tied to poor prognosis in HNSCC (34), in invadopodia formation, and function in HNSCC cells. First, we find that primary HNSCC tumor cells make invadopodia, suggesting that invadopodia are not artifacts of established cultured cell lines. Second, in cortactin-manipulated cells, expression levels of cortactin correlate with both formation of invadopodia, defined as assembly of actin/Arp3 puncta, and associated matrix degradation. However, effects on matrix degradation were more profound. In fact, knocking down cortactin expression was as effective in abolishing ECM degradation at invadopodia sites as the addition of MMP inhibitors, GM6001 or TIMP-2. Third, in cells manipulated for cortactin, it was revealed that secretion of MMP-2 and MMP-9, and surface expression of MT1-MMP, is dependent on the level of cortactin expression.

Cortactin is known as a regulator of branched actin assembly initiated by the Arp2/3 complex. However, it is probably not a primary activator of Arp2/3, but rather a stabilizing factor for branched actin filament networks (29) or a cofactor of WASp family Arp2/3 activators (29, 31, 36, 56, 57). Consistent with those ideas, knockdown cortactin phenotypes are generally described as less pronounced than WASp phenotypes. This, however, depends on the fact that these phenotypes are evaluated almost exclusively on branched actin dynamics, such as in lamellipodial protrusion (36). Therefore, our unexpected finding that in invadopodia the cortactin knockdown phenotype seems to be stronger than N-WASp (14, 15) can be explained by the involvement of cortactin in MMP secretion, in addition to actin dynamics. Consistent with this explanation, siRNA knockdown of other factors known to regulate actin dynamics (e.g., N-WASp, p34Arc, Nck1, and cofilin; ref. 14) did not eliminate ECM degradation, like in cortactin knockdown cells, but only diminished it to the extent that invadopodia formation was decreased.

Invadopodia are thought to be important organelles for cell invasion; however, because the majority of studies have used breast and melanoma cancer cell lines (26, 58–60) it has been controversial whether invadopodia formation is an artifact of cultured cells and whether only limited types of cancers form these structures. Our results with primary HNSCC cultures show that primary tumor cells have the capacity to form invadopodia and broaden the types of cancer cells known to form these structures. Additional experiments are now needed to determine whether HNSCC cancer cells produce invadopodia *in vivo*, and whether they correlate with invasiveness. These experiments will require development of reliable techniques to visualize invadopodia *in vivo*.

We implicated MT1-MMP, MMP-2, and MMP-9 in the cortactin-regulated ECM degradation phenotype. Based on the likely general secretion defect of cortactin knockdown cells, other ECM-degrading proteases could be involved. However, these are strong candidates, based on our MMP inhibitor data as well as studies from other investigators implicating these proteases in invadopodia function (7, 19, 26, 27, 59, 61). Although we detected primarily the zymogen forms of MMP-2 and MMP-9 in conditioned medium, they are likely to be activated on the cell surface by MT1-MMP or other activators (26, 27, 62, 63). It remains to be seen whether this activation occurs predominantly at invadopodia or elsewhere on the cell surface. However, regardless of the site of activation, active MMPs seem to concentrate at invadopodia sites because that is where matrix degradation is readily detectable in our assay. Importantly, MMP-2, MMP-9, and MT1-MMP have all been found to localize to invadopodia (7, 19, 21, 26, 27), and active MMP2 and MMP9 have been found to be associated with either extracts of invadopodia-enriched membrane plus the underlying gelatin substratum (27) or cell membrane extracts (26), respectively.

Secretion of invasive components such as MMPs that are necessary for invadopodia function is likely to occur by trafficking from the *trans*-Golgi network to the plasma membrane (20, 64, 65), consistent with the observed reorientation of the Golgi in close proximity to invadopodia (8). Cortactin could function at several points in this pathway. First, cortactin could be a core part of the secretion machinery, likely involved in vesicle budding and/or movement of vesicles away from the *trans*-Golgi network (41). Such a general role for cortactin in *trans*-Golgi network to plasma membrane trafficking is consistent with our finding that cortactin affects secretion of both MMPs and the non-invadopodia protein ApoA1; that is, constitutive secretion itself seems to be abolished in cortactin knockdown cells. It would also be consistent with the recent finding that a cortactin-dynamin 2 complex regulates trafficking of the VSV-G model protein from the *trans*-Golgi network to the plasma membrane (41). A second possibility, which is not mutually exclusive, is that cortactin may regulate stimulated exocytosis of secretory vesicles containing MMPs, perhaps by tethering them to invadopodia sites where cortactin is concentrated. Indeed, both MT1-MMP and MMP-9 seem to undergo stimulated secretion, for example, in response to concanavalin A and phorbol ester, respectively (63, 64). Finally, it remains to be seen whether these possible roles of cortactin in secretion may synergize mechanistically with its reported role in favoring actin assembly and/or signaling in invadopodia (7, 10, 28, 42). Future studies should address the exact mechanism(s) by which cortactin regulates secretion. For example, it is not clear why overexpression of cortactin leads to a significant increase in the secretion of all three MMPs examined in this study but not of ApoA1. These in-depth analyses are worthwhile because they may shed light on basic mechanisms underlying the correlation between increased expression of cortactin and poor prognosis observed in patients with HNSCC (33, 34).

Artym et al. (7) did a detailed analysis of invadopodia formation, including live cell imaging of tagged cortactin and MT1-MMP molecules. Based on those studies, they proposed a stepwise model of invadopodia formation in which cortactin is initially recruited to and marks early-stage invadopodia, followed by accumulation of MT1-MMP and ECM degradation. Our data are consistent with that model, but suggest that the primary role of cortactin in early-stage invadopodia may be to deliver MMPs for ECM degradation rather than to regulate actin dynamics. Similar to our finding with MMP inhibitors, Artym et al. (7) also found a decrease in invadopodia formation by inhibiting MT1-MMP with siRNA, supporting the idea that MMP activity in the extracellular space leads to new signals for invadopodia formation. The nature of the feedback signal is currently unknown, but might include activation of latent growth factors or other growth-mimicking products of ECM degradation.

In summary, we propose a model in which cortactin promotes the secretion of MMPs necessary for ECM degradation at invadopodia. Positive feedback from MMP degradation products may further drive the system to initiate formation of new invadopodia. Although cortactin is still likely to play a role in actin dynamics at invadopodia, the essential function in MMP secretion described here seems to drive high levels of ECM degradation and may provide one explanation for the association of cortactin overexpression with poor prognosis in HNSCC and other cancers.

Acknowledgments

Received 10/24/2006; revised 2/5/2007; accepted 2/27/2007.

Grant support: NIH K22 CA109590-01 and American Cancer Society RSG CSM 112364 grants (A.M. Weaver), and funding from the Barry Baker Laboratory for Head and Neck Oncology, the Kleberg Foundation, and the Vanderbilt Ingram Cancer Center (W.G. Yarbrough).

The costs of publication of this article were defrayed in part by the payment of page charges. This article must therefore be hereby marked *advertisement* in accordance with 18 U.S.C. Section 1734 solely to indicate this fact.

We thank Hideki Yamaguchi, John Condeelis, Barbara Fingleton, and Jerome Jourquin for technical advice; Lynn Matrisian and Vito Quaranta for critical reading of the manuscript; and Susette Mueller for general collegiality and support. Experiments were done in part through the use of the Vanderbilt University Medical Center Flow Cytometry core and the Vanderbilt University Medical Center Cell Imaging Shared Resource.

References

1. Hoon DS, Kitago M, Kim J, et al. Molecular mechanisms of metastasis. Cancer Metastasis Rev 2006;25:203–20.
2. Pantel K, Brakenhoff RH. Dissecting the metastatic cascade. Nat Rev Cancer 2004;4:448–56.
3. Chen WT, Chen JM, Parsons SJ, Parsons JT. Local degradation of fibronectin at sites of expression of the transforming gene product pp60src. Nature 1985;316:156–8.
4. Weaver AM. Invadopodia: specialized cell structures for cancer invasion. Clin Exp Metastasis 2006;23:97–105.
5. Linder S, Aepfelbacher M. Podosomes: adhesion hotspots of invasive cells. Trends Cell Biol 2003;13:376–85.
6. Baldassarre M, Ayala I, Beznoussenko G, et al. Actin dynamics at sites of extracellular matrix degradation. Eur J Cell Biol 2006;85:1217–31.
7. Artym VV, Zhang Y, Seillier-Moiseiwitsch F, Yamada KM, Mueller SC. Dynamic interactions of cortactin and membrane type 1 matrix metalloproteinase at invadopodia: defining the stages of invadopodia formation and function. Cancer Res 2006;66:3034–43.
8. Baldassarre M, Pompeo A, Beznoussenko G, et al. Dynamin participates in focal extracellular matrix degradation by invasive cells. Mol Biol Cell 2003;14:1074–84.
9. Bowden ET, Barth M, Thomas D, Glazer RI, Mueller SC. An invasion-related complex of cortactin, paxillin and PKCμ associates with invadopodia at sites of extracellular matrix degradation. Oncogene 1999;18:4440–9.
10. Bowden ET, Onikoyi E, Slack R, et al. Co-localization of cortactin and phosphotyrosine identifies active invadopodia in human breast cancer cells. Exp Cell Res 2006;312:1240–53.
11. Chellaiah MA. Regulation of podosomes by integrin $\alpha_v\beta_3$ and Rho GTPase-facilitated phosphoinositide signaling. Eur J Cell Biol 2006;85:311–7.
12. Kaverina I, Stradal TE, Gimona M. Podosome formation in cultured A7r5 vascular smooth muscle cells requires Arp2/3-dependent *de novo* actin polymerization at discrete microdomains. J Cell Sci 2003;116:4915–24.
13. Spinardi L, Rietdorf J, Nitsch L, et al. A dynamic podosome-like structure of epithelial cells. Exp Cell Res 2004;295:360–74.
14. Yamaguchi H, Lorenz M, Kempiak S, et al. Molecular mechanisms of invadopodium formation: the role of the N-WASP-Arp2/3 complex pathway and cofilin. J Cell Biol 2005;168:441–52.
15. Yamaguchi H, Condeelis J. Regulation of the actin cytoskeleton in cancer cell migration and invasion. Biochim Biophys Acta. In press, doi:10.1016.2006.

16. Stetler-Stevenson WG, Hewitt R, Corcoran M. Matrix metalloproteinases and tumor invasion: from correlation and causality to the clinic. Semin Cancer Biol 1996; 7:147.
17. Rosenthal EL, Matrisian LM. Matrix metalloproteases in head and neck cancer. Head Neck 2006;28:639–48.
18. Ayala I, Baldassarre M, Caldieri G, Buccione R. Invadopodia: a guided tour. Eur J Cell Biol 2006;85: 159–64.
19. Chen WT, Wang JY. Specialized surface protrusions of invasive cells, invadopodia and lamellipodia, have differential MT1-MMP, MMP-2, and TIMP-2 localization. Ann N Y Acad Sci 1999;878:361–71.
20. Mazzone M, Baldassarre M, Beznoussenko G, et al. Intracellular processing and activation of membrane type 1 matrix metalloprotease depends on its partitioning into lipid domains. J Cell Sci 2004;117:6275–87.
21. Nakahara H, Howard L, Thompson EW, et al. Transmembrane/cytoplasmic domain-mediated membrane type 1-matrix metalloprotease docking to invadopodia is required for cell invasion. Proc Natl Acad Sci U S A 1997;94:7959–64.
22. Chen WT, Kelly T. Seprase complexes in cellular invasiveness. Cancer Metastasis Rev 2003;22:259–69.
23. Hernandez-Barrantes S, Bernardo M, Toth M, Fridman R. Regulation of membrane type-matrix metalloproteinases. Semin Cancer Biol 2002;12:131–8.
24. Chakraborti S, Mandal M, Das S, Mandal A, Chakraborti T. Regulation of matrix metalloproteinases: an overview. Mol Cell Biochem 2003;253:269–85.
25. Das S, Mandal M, Chakraborti T, Mandal A, Chakraborti S. Structure and evolutionary aspects of matrix metalloproteinases: a brief overview. Mol Cell Biochem 2003;253:31–40.
26. Bourguignon LY, Gunja-Smith Z, Iida N, et al. CD44v(3,8-10) is involved in cytoskeleton-mediated tumor cell migration and matrix metalloproteinase (MMP-9) association in metastatic breast cancer cells. J Cell Physiol 1998;176:206–15.
27. Monsky WL, Kelly T, Lin CY, et al. Binding and localization of M(r) 72,000 matrix metalloproteinase at cell surface invadopodia. Cancer Res 1993;53:3159–64.
28. Webb BA, Eves R, Mak AS. Cortactin regulates podosome formation: roles of the protein interaction domains. Exp Cell Res 2006;312:760–9.
29. Weaver AM, Karginov AV, Kinley AW, et al. Cortactin promotes and stabilizes Arp2/3-induced actin filament network formation. Curr Biol 2001;11:370–4.
30. Wu H, Parsons JT. Cortactin, an 80/85-kilodalton pp60src substrate, is a filamentous actin-binding protein enriched in the cell cortex. J Cell Biol 1993;120:1417–26.
31. Uruno T, Liu J, Zhang P, et al. Activation of Arp2/3 complex-mediated actin polymerization by cortactin. Nat Cell Biol 2001;3:259–66.
32. Daly RJ. Cortactin signalling and dynamic actin networks. Biochem J 2004;382:13–25.
33. Patel AM, Incognito LS, Schechter GL, Wasilenko WJ, Somers KD. Amplification and expression of EMS-1 (cortactin) in head and neck squamous cell carcinoma cell lines. Oncogene 1996;12:31–5.
34. Rodrigo JP, Garcia LA, Ramos S, Lazo PS, Suarez C. EMS1 gene amplification correlates with poor prognosis in squamous cell carcinomas of the head and neck. Clin Cancer Res 2000;6:3177–82.
35. Freier K, Sticht C, Hofele C, et al. Recurrent coamplification of cytoskeleton-associated genes EMS1 and SHANK2 with CCND1 in oral squamous cell carcinoma. Genes Chromosomes Cancer 2006;45:118–25.
36. Bryce NS, Clark ES, Leysath JL, et al. Cortactin promotes cell motility by enhancing lamellipodial persistence. Curr Biol 2005;15:1276–85.
37. Patel AS, Schechter GL, Wasilenko WJ, Somers KD. Overexpression of EMS1/cortactin in NIH3T3 fibroblasts causes increased cell motility and invasion *in vitro*. Oncogene 1998;16:3227–32.
38. Rothschild BL, Shim AH, Ammer AG, et al. Cortactin overexpression regulates actin-related protein 2/3 complex activity, motility, and invasion in carcinomas with chromosome 11q13 amplification. Cancer Res 2006;66: 8017–25.
39. Helwani FM, Kovacs EM, Paterson AD, et al. Cortactin is necessary for E-cadherin-mediated contact formation and actin reorganization. J Cell Biol 2004;164: 899–910.
40. Sauvonnet N, Dujeancourt A, Dautry-Varsat A. Cortactin and dynamin are required for the clathrin-independent endocytosis of γc cytokine receptor. J Cell Biol 2005;168:155–63.
41. Cao H, Weller S, Orth JD, et al. Actin and Arf1-dependent recruitment of a cortactin-dynamin complex to the Golgi regulates post-Golgi transport. Nat Cell Biol 2005;7:483–92.
42. Tehrani S, Faccio R, Chandrasekar I, Ross FP, Cooper JA. Cortactin has an essential and specific role in osteoclast actin assembly. Mol Biol Cell 2006;17: 2882–95.
43. Yarar D, To W, Abo A, Welch MD. The Wiskott-Aldrich syndrome protein directs actin-based motility by stimulating actin nucleation with the Arp2/3 complex. Curr Biol 1999;9:555–8.
44. Brummelkamp TR, Bernards R, Agami R. Stable suppression of tumorigenicity by virus-mediated RNA interference. Cancer Cell 2002;2:243–7.
45. Ireton RC, Davis MA, van Hengel J, et al. A novel role for p120 catenin in E-cadherin function. J Cell Biol 2002; 159:465–76.
46. Weichselbaum RR, Dahlberg W, Beckett M, et al. Radiation-resistant and repair-proficient human tumor cells may be associated with radiotherapy failure in head- and neck-cancer patients. Proc Natl Acad Sci U S A 1986;83:2684–8.
47. Whigham A, Netterville J, Burkey B, et al. Short-term culture and *in vivo* modeling of primary head and neck squamous cell carcinoma. Arch Otolaryngol Head Neck Surg 2006;132:901–2.
48. Chen W-T, Yunyon Y, Nakahara H. An *in vitro* cell invasion assay: determination of cell surface proteolytic activity that degrades extracellular matrix. J Tissue Cult Methods 1994;16:177–81.
49. Brabek J, Constancio SS, Shin NY, et al. CAS promotes invasiveness of Src-transformed cells. Oncogene 2004;23: 7406–15.
50. Brabek J, Constancio SS, Siesser PF, et al. Crk-associated substrate tyrosine phosphorylation sites are critical for invasion and metastasis of SRC-transformed cells. Mol Cancer Res 2005;3:307–15.
51. Franzke CW, Tasanen K, Schacke H, et al. Transmembrane collagen XVII, an epithelial adhesion protein, is shed from the cell surface by ADAMs. EMBO J 2002;21: 5026–35.
52. Seals DF, Courtneidge SA. The ADAMs family of metalloproteases: multidomain proteins with multiple functions. Genes Dev 2003;17:7–30.
53. Mbeunkui F, Fodstad O, Pannell LK. Secretory protein enrichment and analysis: an optimized approach applied on cancer cell lines using 2D LC-MS/MS. J Proteome Res 2006;5:899–906.
54. Coussens LM, Fingleton B, Matrisian LM. Matrix metalloproteinase inhibitors and cancer: trials and tribulations. Science 2002;295:2387–92.
55. Chin D, Boyle GM, Porceddu S, et al. Head and neck cancer: past, present and future. Expert Rev Anticancer Ther 2006;6:1111–8.
56. Weaver AM, Heuser JE, Karginov AV, et al. Interaction of cortactin and N-WASp with Arp2/3 complex. Curr Biol 2002;12:1270–8.
57. Weaver AM, Young ME, Lee WL, Cooper JA. Integration of signals to the Arp2/3 complex. Curr Opin Cell Biol 2003;15:23–30.
58. Kelly T, Yan Y, Osborne RL, et al. Proteolysis of extracellular matrix by invadopodia facilitates human breast cancer cell invasion and is mediated by matrix metalloproteinases. Clin Exp Metastasis 1998;16:501–12.
59. Monsky WL, Lin CY, Aoyama A, et al. A potential marker protease of invasiveness, seprase, is localized on invadopodia of human malignant melanoma cells. Cancer Res 1994;54:5702–10.
60. Nakahara H, Nomizu M, Akiyama SK, et al. A Mechanism for regulation of melanoma invasion. Ligation of $\alpha_6\beta_1$ integrin by laminin G peptides. J Biol Chem 1996;271:27221–4.
61. Deryugina EI, Ratnikov B, Monosov E, et al. MT1-MMP initiates activation of pro-MMP-2 and integrin $\alpha v\beta 3$ promotes maturation of MMP-2 in breast carcinoma cells. Exp Cell Res 2001;263:209–23.
62. Sato H, Takino T, Kinoshita T, et al. Cell surface binding and activation of gelatinase A induced by expression of membrane-type-1-matrix metalloproteinase (MT1-MMP). FEBS Lett 1996;385:238–40.
63. Zucker S, Hymowitz M, Conner CE, DiYanni EA, Cao J. Rapid trafficking of membrane type 1-matrix metalloproteinase to the cell surface regulates progelatinase a activation. Lab Invest 2002;82:1673–84.
64. Williger B-T, Ho W-T, Exton JH. Phospholipase D mediates matrix metalloproteinase-9 secretion in phorbol ester-stimulated human fibrosarcoma cells. J Biol Chem 1999;274:735–8.
65. Sternlicht MD, Werb Z. How matrix metalloproteinases regulate cell behavior. Annu Rev Cell Dev Biol 2001;17:463–516.